



OPEN Development of a multi-layer high-efficiency GEM-based neutron detector for spallation sources

S. Cancelli^{1,2,3}✉, F. Caruggi¹, E. Perelli Cippo³, O. Putignano³, A. Celora¹, G. Gorini^{1,2}, M. Krzystyniak⁴, A. Muraro⁴, G. Romanelli^{4,5}, R. S. Pinna⁶, M. Tardocchi³ & G. Croci^{1,2,3}

Neutron detection is nowadays mostly based on ^3He gas detectors, but its shortage and the continuous upgrades of the neutron facilities require new devices to perform experiments with maximum performances. This work presents a new detector based on the Gas Electron Multiplier (GEM) combined with several boron layers. This detector combines the features of GEM technology with the properties of boron as a neutron converter and the device is produced to sustain high neutron fluxes with high detection efficiency. The detector has been characterised at the ISIS Pulsed Neutron and Muon Source (UK). Based on the analysis of our results, the detector has shown a good response to thermal and epithermal neutrons reaching a detection efficiency of 16% at 1.8 Å (25 meV). The good detection efficiency (even increasable with the addition of further boron GEM foils) and the good time resolution, make the detector a unique device for the neutron techniques. In particular, its use can easily be envisaged in techniques involving neutron transmission measurements, that require high fluxes impinging on the detectors, with the added bonus of a 2D-resolved capability due to the padded anode.

The state of the art of thermal neutron detection is based on the ^3He gas tube (detecting neutrons through, the $^3\text{He}(n,p)^3\text{H}$ nuclear reaction thanks to its high cross section¹) but during the last ten years the ^3He shortage², due to its use for nuclear safety, has brought the necessity to develop new neutron detectors with comparable characteristics. Moreover, the new Spallation Sources under construction, such as the European Spallation Source (ESS) in Sweden, will provide a neutron flux of 10^9 n/cm²s at the detector; thus, detectors capable to sustain neutron fluxes in this order of magnitude are required. ^3He gas tubes have a high detection efficiency (90% at thermal neutron energies thanks to the high cross section of the involved neutron reaction) but their counting rates are typically limited to kHz/cm²³. In these conditions, ^3He tubes used as a detector in transmission geometry (where the largest fraction of neutrons would be directed) could not make a good use of the high available fluxes in ESS.

An alternative can be found on the Gas Electron Multiplier (GEM) detectors when coupled with a suitable neutron “converter”; in fact, GEMs are basically charged-particle detectors and they are made sensitive to neutral particles when they interact in a suitable material with the emission of charged products.

GEM detectors were developed for the first time at CERN in 1997 by Sauli⁴ and the main component is represented by the GEM foil, an insulating layer covered on both sides with a conductive layer and then micro-perforated with high density (50–100 holes/mm²). The geometrical structure allows to reach a high voltage inside the GEM foil holes so that the resulting electric field inside the micro-holes is high enough to trigger electron multiplication in the gas saturating the device⁴ when a suitable ΔV is applied to the conductive layers. The GEM foils are stacked between a cathode and an anode and the system is filled with a gas mixture, usually Ar-CO₂ with relative volume concentrations of 70–30%, respectively.

Inserting a single boron layer inside a GEM detector assembly, thermal neutrons can be detected. A detector of this kind has been developed depositing a $^{10}\text{B}_4\text{C}$ layer on the GEM cathode and the reached detection efficiency for 25 meV neutrons resulted to be 1%⁵.

The first boron GEM foil was produced by the CASCADE group of the Heidelberg University in 2011⁶. The group developed a setup characterised by a strip anode placed in the middle of the detector and six 20×20 cm²

¹Università degli Studi Milano-Bicocca, Piazza dell’Ateneo Nuovo 1, 20126 Milan, Italy. ²Sezione Milano-Bicocca, Istituto Nazionale Fisica Nucleare, Piazza della Scienza 3, 20126 Milan, Italy. ³Istituto per la Scienza e la Tecnologia dei Plasmi – CNR, Via Cozzi 53, 20126 Milan, Italy. ⁴ISIS Neutron and Muon Source, RAL, Didcot, Oxfordshire OX11 0QX, UK. ⁵Dipartimento di Fisica and NAST Centre, Università degli Studi di Roma Tor Vergata, Via Della Ricerca Scientifica, 00133 Rome, Italy. ⁶ENI, Via Emilia, 1 e Piazza Ezio Vanoni, 1, 20097 San Donato Milanese, (MI), Italy. ✉email: stephanie.cancelli@unimib.it

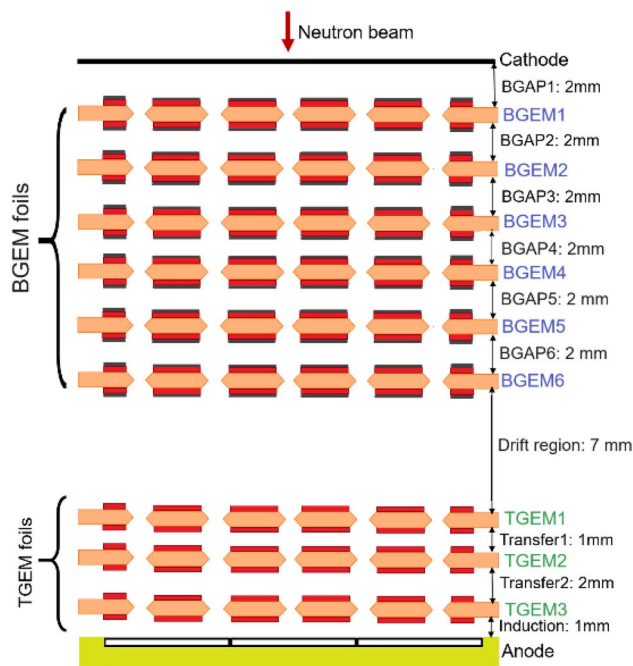


Fig. 1. The I-MS-BGEM scheme.

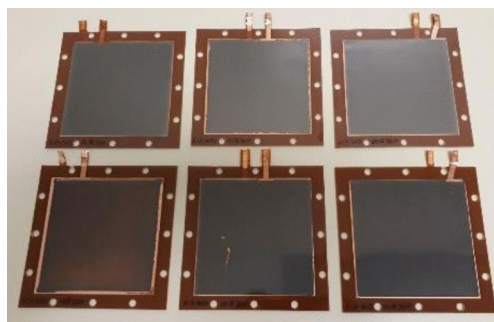


Fig. 2. Picture of the six BGEM foils.

GEM foils (each with a single boron layer) were positioned on the two sides of the anode. With this configuration the detection efficiency of thermal neutrons was around 21%, depending on the different layer thicknesses (between 0.8 and 1 μm)⁷. Despite these promising results, a double boron coating on the two sides of each GEM foil was not possible at the time⁷.

Recent works have shown that the optimal thickness for a single boron layer is 1 μm ⁸, due to the concurring effects of neutron capture and charged products escape probability. The detection efficiency can thus be increased by depositing 1 μm thick $^{10}\text{B}_4\text{C}$ layers directly on the both sides of a $3 \times 3 \text{ cm}^2$ GEM foil creating a boron-GEM (BGEM) foil⁹, demonstrating that the counting rate is linear just with the number of added double layers (up to six).

Based on this idea the present Improved Medium-Size BGEM (I-MS-BGEM) detector has been designed and realised with the aim of reaching an efficiency in the order of 20% to thermal neutrons but with a sustainable counting rate of MHz/mm^2 .

The main component of the I-MS-BGEM is the stack (shown in Fig. 1) of 6 BGEM foils (12 boron layers) as (Fig. 2), which is coupled with a triple GEM (TGEM: a typical arrangement of three standard GEM foils)¹⁰. The BGEM stack is necessary to convert thermal neutrons into charged particles through the nuclear reaction $^{10}\text{B}(n,\alpha)^7\text{Li}$; thus, the alpha and lithium particles can escape from it and ionise the gas⁸. The applied High Voltage (HV) to each layer of the BGEM stack creates an electric field intense enough transport through the BGEM foils micro-holes only the electrons arising from the gas ionisation. The applied HV to the TGEM foils, however is so high (250–500 V) that in the micro-holes of the TGEM electron multiplication occurs, so that the final number of electrons impinging the anode give a detectable signal¹⁰.

The device has been characterised at the ISIS Pulsed Neutron and Muon Source¹¹ at the VESUVIO beamline^{12,13}, where neutrons in the thermal and epithermal energy range are available; the characterisation was

performed to provide: the detector stability, the capability to discriminate neutrons from gamma-rays and the detection efficiency.

Detector realisation and experimental setup

The I-MS-BGEM detector has been built up stacking a cathode, six BGEM foils, three standard GEM foils and a padded anode with $256 \times 6 \times 6 \text{ mm}^2$ pads (Fig. 1).

The BGEM foils (Fig. 2) manufacturing is based on a modification of the standard GEM foil realisation process. The entire production process is accurately described in⁹, but for completeness the following paragraph reports a summarise of the process.

The GEM foil raw material (50 μm -thick polyimide foil coated on both sides with 5 μm of copper) was treated at CERN¹⁴, where the standard pattern of the holes (diameter of 70 μm and pitch 140 μm) was designed on a square of $10 \times 10 \text{ cm}^2$ on the top and on the bottom of the foil. This was followed by the photoresist lamination on both faces, with photoresist dots precisely covering the copper openings, and then curing. Subsequently, these foils were individually placed between two aluminium masks with $10 \times 10 \text{ cm}^2$ openings on each face, aligned with the patterned active areas on both sides of the foil, at the University of Milano Bicocca. The $^{10}\text{B}_4\text{C}$ deposition was performed by the European Spallation Source Coating Group¹⁵ and, after a first etching, the foils were positioned in a deposition chamber (with a pressure of $1.5 \times 10^{-4} \text{ Pa}$) and coated with a $^{10}\text{B}_4\text{C}$ layer in pure argon at 0.40 Pa and with a Cu capping layer in pure layer at 0.30 Pa without breaking the vacuum⁹. The chemical composition of the $^{10}\text{B}_4\text{C}$ layer was analysed using elastic recoil detection analysis at Uppsala University's Tandem Laboratory and the analysis showed a relative atomic ratio of approximately 77% B, 18% C, and 5% impurities (mainly O and H). After the boron deposition, the GEM foils were returned to CERN for final processing and etching. The photoresist dots were removed from the foils to etch the polyimide, which was masked at this stage by the boron deposition. Following this procedure for creating the holes, the foils show the usual GEM pattern in the central area on both faces and copper cladding on the outer surface. The average $^{10}\text{B}_4\text{C}$ thickness on both sides was found to be around 1 μm .

The assembled detector was equipped with the GEMINI (GEM INtegrated Interface)¹⁶ system, a custom digital electronic readout designed for GEM detectors. GEMINI is an ASIC made of 16 readout channels, which converts the charge signal from the anode pads (each pad is a channel) into a voltage signal proportional to the Time over Threshold (ToT) i.e. the amount of time the input analog signal spent over the threshold level (a custom threshold is set for each channel separately). The signals are then digitized by an ADC and sent via optical fibre to the DAQ computer; for each event, along with the ToT, the ID of the channel and the timestamp (related to the Time of Arrival of the particle) are stored. The theoretical time resolution of the device is dominated by the length of the induction signal on the anode pads, which is in the order of a few ns; thus the detector can sustain counting rates in the order of 1 MHz/cm²¹⁷.

The detector has been characterized at ISIS, where neutrons are produced from the collision between 800 MeV proton bunches and a tantalum-tungsten spallation target¹⁸. After the spallation, neutrons are emitted with all energies up to 800 MeV, thus a series of moderators are located around the target to slow down the fast neutrons. The neutrons are redirected towards the experimental stations (block-houses) and the I-MS-BGEM has been placed in transmission position in the VESUVIO block-house, in Target Station 1.

VESUVIO is a so-called inverted-geometry spectrometer¹⁹, which provides neutrons in all energy ranges, from cold neutrons (meV) to fast neutrons (MeV), but it is optimised to perform spectroscopy experiments, respectively, in the thermal and epithermal (25 meV–100 eV) energy range; an important feature for the present characterisation is that its configuration (see Fig. 3) also allows to take measurements in transmission geometry. This feature is useful for experiments aimed to determine, for example, neutron cross-sections of biological molecules¹³. The obtained information is important to improve the neutron cross sections database of molecules for the benefit of the scientific community²⁰. The I-MS-BGEM detector has been positioned between the VESUVIO sample holder and the ^6Li -based²¹ VESUVIO transmission beam monitor at a distance $L = 12.3 \text{ m}$ from the moderator.

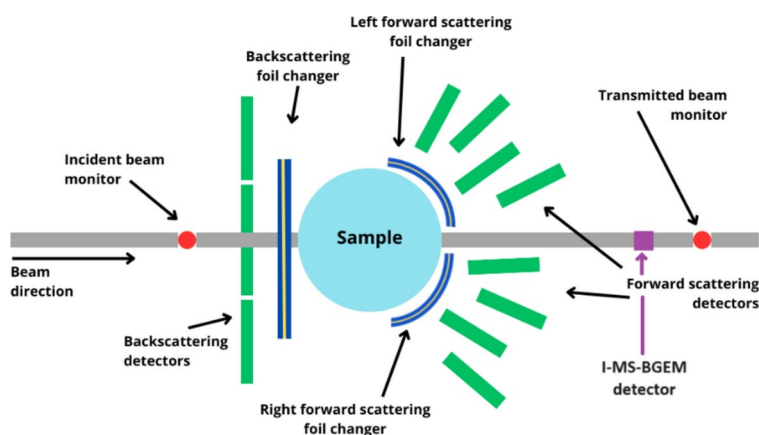


Fig. 3. Schematics of the VESUVIO beamline.

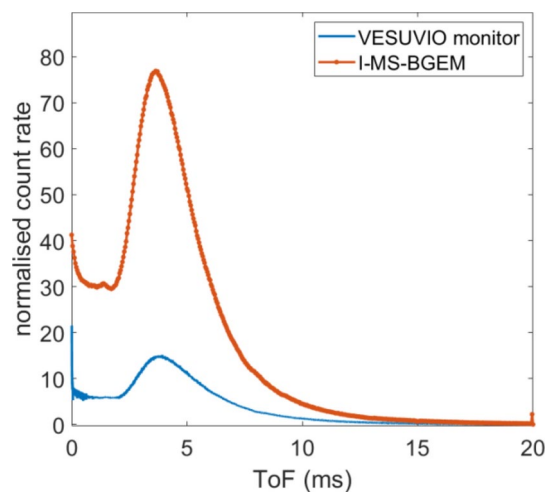


Fig. 4. ToF spectra normalised for the time measurement (count rate) and for the proton beam current obtained with the I-MS-BGEM detector (orange-dot plot) and with the VESUVIO monitor (blue line) respectively.

The time difference between the neutron production time, usually called t_0 “start signal”, and the time of the charged particles collection (the arrival time obtained by the GEMINI readout for every detected neutron) is defined as the Time of Flight (ToF), from which the incident neutron energies E_n can be obtained with:

$$E_n = \frac{1}{2} m_n \frac{L^2}{T_{oF}^2} \quad (1)$$

where m_n is the neutron mass.

Results and discussion

Figure 4 shows the ToF spectra of an open beam measurement obtained with the I-MS-BGEM detector and with the standard VESUVIO transmission monitor, normalised to the proton beam current and the measurement duration. Both spectra feature a peak between 3 and 4 ms (milliseconds) corresponding to the peak of the Maxwell-Boltzman distribution for thermalized neutrons in the water moderator serving the instrument. At ToF lower than 100 μ s, the gamma efficiency of the standard scintillating monitor makes the spectra affected by a gamma background, related to neutron activation and prompt-gammas within the blockhouse and in the

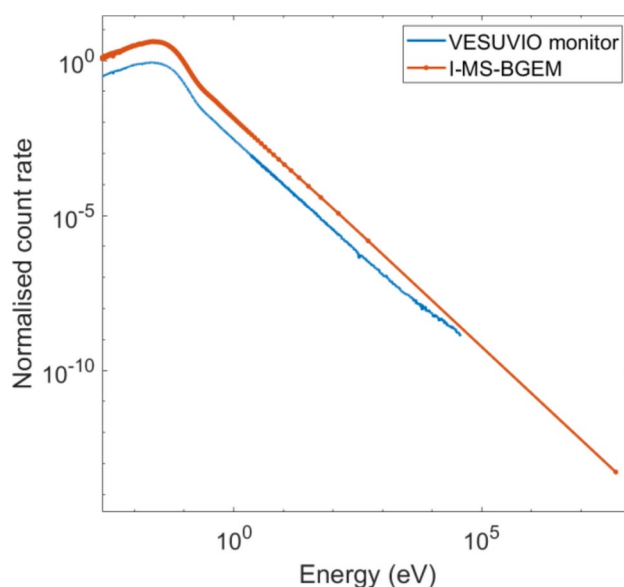


Fig. 5. Energy spectra normalised for the time measurement and for the proton beam current obtained with the I-MS-BGEM detector (orange-dot plot) and with the VESUVIO monitor (blue line) respectively.

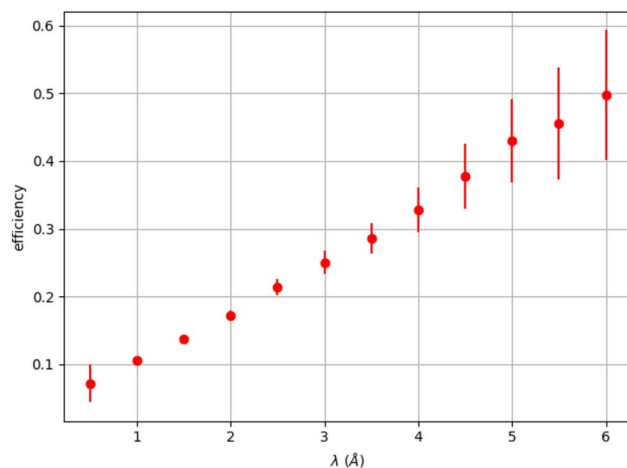


Fig. 6. Detection efficiency for different wavelengths estimated with the formula 2. Error bars just reflect the statistical (Poisson) nature of the uncertainty, being smaller in the thermal region where the number of detected neutrons is higher.

beam-stop. At ToF values lower than 5 μ s, spectra are rarely collected by the standard detector, because of the presence of the so-called gamma flash from the target-reflector-moderator assembly. In fact, it is known that the spallation process also produces a highly intense burst of gamma rays and fast, unmoderated neutrons that propagate through the neutron beam pipes and may reach the detectors of the different block-houses. Being much faster than thermal neutrons, such gamma rays “accumulate” in the shortest time region of the ToF spectrum. Although they are usually not relevant for detector positioned in scattering geometry (as the majority of detectors even in the VESUVIO beamline), they can affect both incidence and transmission monitors, that are positioned directly in the beam. As a result, data collected by standard monitors (like for instance scintillation-based monitors) in the very low ToF region (for instance, at VESUVIO, in the region $\text{ToF} < 0.1$ ms) are affected by a high background. The I-MS-BGEM, on the other hand, is insensitive to gamma rays (see further for details) thus the counts collected in this region really reflect the distribution of fast neutrons, as it is clearly visible in Figs. 4 and 5.

ToF spectra can be easily transformed (with the use of the Eq. 1) into the energy spectra, reported in Fig. 5.

The detector characterization performed at ISIS has been focused on the determination: the detector efficiency, the capability to discriminate gamma rays from neutrons and the stability during a long measurement time.

The detection efficiency has been estimated considering two wavelength spectra obtained with the I-MS-BGEM and with the VESUVIO monitor, that is credited with an efficiency $\varepsilon_{\text{VESUVIO}} = 0.6\%$ at 1 Å neutron wavelength²².

The efficiency of the I-MS-BGEM has been calculated making use of the following formula:

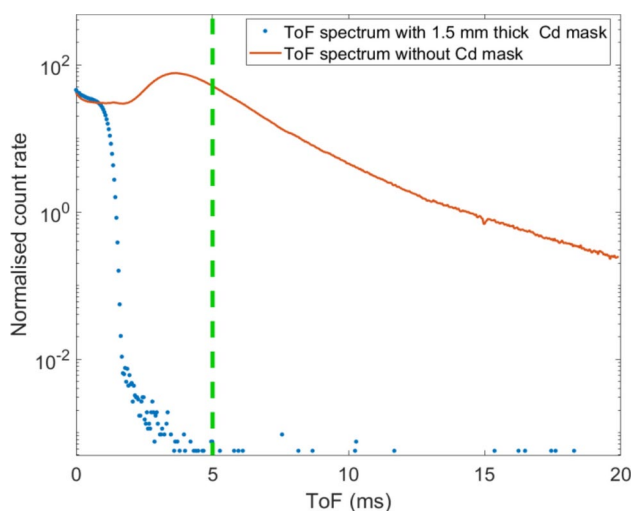


Fig. 7. Overlap of two ToF spectra. The orange plot indicates the ToF spectrum obtained with the empty sample-holder. The blue one is the ToF spectrum of a Cadmium sample; in fact, the drop at 1.3 ms is due to the resonance at 0.5 eV, which absorbs all neutrons below this energy.

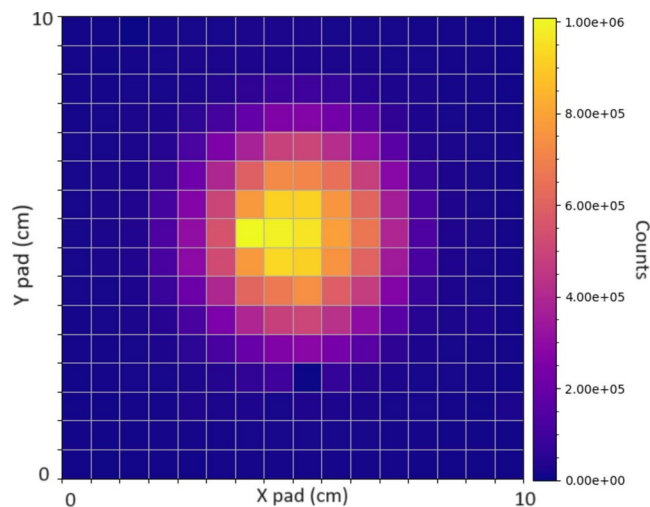


Fig. 8. 2D spatial map of the VESUVIO neutron beam profile. Considering the inner six pads along X and Y, a beam profile of $3.5 \times 3.5 \text{ cm}^2$ is displayed, comparable with other measurements²².

$$\varepsilon_{I-MS-BGEM} = \frac{\text{counts}(\lambda, I-MS-BGEM)}{\text{counts}(\lambda, VESUVIO \text{ monitor})} * \varepsilon_{VESUVIO} \quad (2)$$

Figure 6 shows the detection efficiency trend for different wavelength intervals; it increases with the neutron wavelength from 8% at 0.5 \AA up to 50% at 6 \AA , as it is expected in the ideal case in which the efficiency is only due to the probability of neutron “conversion” in boron, without saturation effects or losses of signal (due for instance to the physical dimensions of the detector or loss of electrons during transport from the different sensitive layers). The error bars have been calculated with the error propagation and the different widths are due to the lower statistics at long wavelength (visible in the left side of the graph in Fig. 5). This detection efficiency combined with the low gamma-sensitivity allows to explore different wavelength regions within the same measurement, thus reducing the exposure time of the samples to neutrons. These performances are especially promising when using the detector in transmission geometry, for instance to determine the total neutron cross sections of organic molecules and biological specimens. As a matter of fact, a GEM detector with a single boron layer had already been used on the VESUVIO beamline²² and in the same position of the I-MS-BGEM to measure total neutron cross sections of a series of amino acids²³. On this occasion the detector had reached a detection efficiency of 1% at thermal neutron energy, requiring irradiation times in the order of a few hours for every single specimen to obtain a reasonable statistic. With the present I-MS-BGEM, which increased efficiency to 16%, the measurement time would be significantly reduced, thus providing the possibility to investigate more samples within the same experimental time, or to investigate specimens (like for instance biological specimens or catalysts) that are subject to quick degradation.

Moreover, each boron layer with a thickness $1 \mu\text{m}$ (as in our case) provides a detection efficiency of about 1.2%: this was verified during the tests while activating BGEM foils one by one. This test did not show any sign of saturation or linearity in the efficiency as already proved by previous tests described in⁹. The present detector

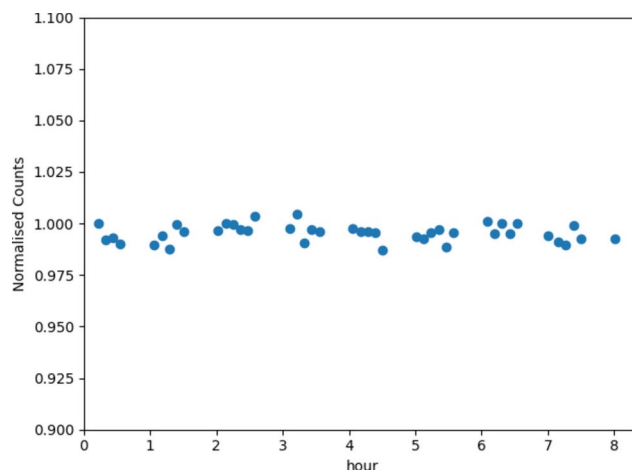


Fig. 9. A run series considered to estimate the I-MS-BGEM stability during time.

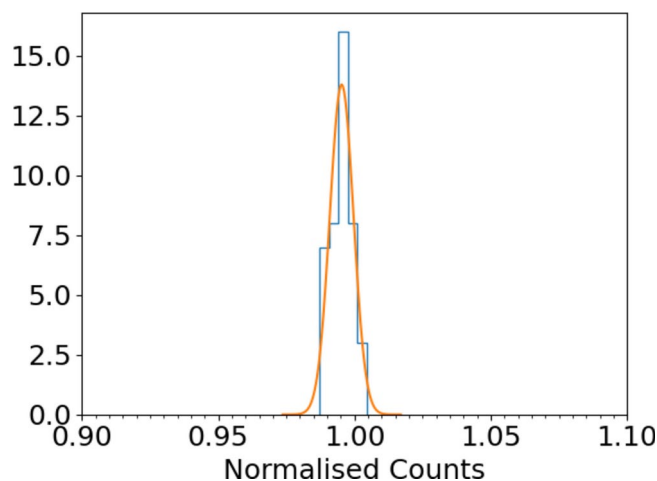


Fig. 10. Plot of the histogram considering the points reported inside Fig. 9. From the Gaussian fit, the centroid is 0.995 and the standard deviation is 0.003.

is made of six BGEM foils, but more BGEMs can be stacked to increase the detection efficiency. For instance, a stack of 20 BGEM foils can achieve a detection efficiency in the order of 50% at 1.8 Å, with the bonus of a higher rate capability respect to ^3He gas tubes.

The detector capability to discriminate events due to gamma rays from neutrons has been studied with the use of a 1.5 mm thick Cadmium mask inserted inside the sample holder at the centre of the neutron beam (see Fig. 3). Cadmium has a neutron cross-section with a wide absorption resonance between 0.1 and 0.5 eV²⁴ and neutrons with this energy range have approximately 100% probability to be absorbed in the Cd foil. As a consequence, it acts roughly as a “high-pass filter”, absorbing most of the neutrons with energies below 0.5 eV.

Figure 7 compares a spectrum obtained with I-MS-BGEM using the named Cd filter (orange line) and without the filter (blue dots). It is visible in the “filtered” spectrum a drop at about 1.3 ms (marked by the green dashed line), which corresponds to the energy value of 0.5 eV; counts registered in the detector below this energy (due either to gamma rays or residual neutrons crossing the filter) are roughly 5 orders of magnitude lower than counts above it. If we consider for sake of simplicity that all such counts are due to gamma rays, the gamma-neutron discrimination capability γ_{factor} can be estimated considering the total counts for the (5–19 ms) ToF region for the spectrum with the Cd filter and the counts in the same interval of the spectrum without the filter:

$$\gamma_{\text{factor}} = \frac{\text{counts of the filtered region (5 ms - 20ms)}}{\text{counts ToF (5ms - 20ms) of a reference run}} = (1.07 \pm 0.05) * 10^{-5} \frac{\gamma}{n} \quad (3)$$

The region of interest ranges from 5 to 19 ms, to avoid considering neutrons which pass through the Cd filter.

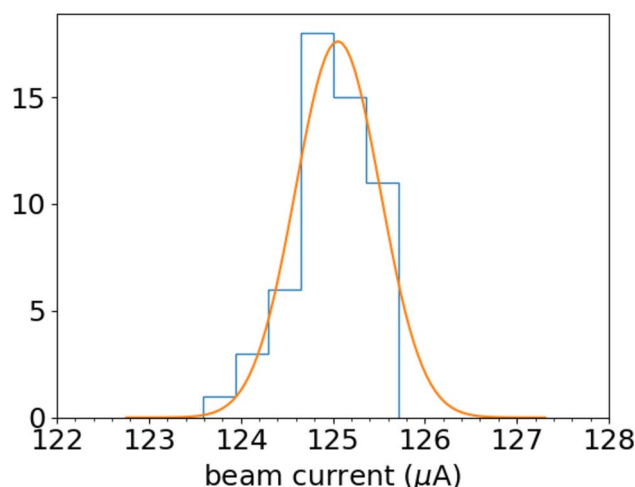


Fig. 11. Plot of the histogrammed data relative to the proton beam current values. From the Gaussian fit, the centroid is 125 μA and the standard deviation is 0.445.

Detector	Efficiency at thermal neutrons (%)	Count rate capability
³ He tubes	90	kHz
⁶ Li scintillator	1.1	MHz
I-MS-BGEM	16	MHz

Table 1. Comparison of the ³He, ⁶Li and I-MS-BGEM features.

The padded anode allows to obtain an image of the VESUVIO neutron beam profile (Fig. 8); in the present detector, the spatial resolution is limited by the pad dimension ($6 \times 6 \text{ mm}^2$); to improve this value, smaller pads or strips are needed, at the cost of increasing the number of channels and electronics.

The BGEMs stack introduces an uncertainty in the ToF measurement due to the fact that two neutrons with the same energy can be converted in a different part of the stack. This effect is common on all detectors which the active area is a volume and not a surface. Considering the BGEM stack thickness (1.2 cm), the maximum ToF spread is 15 μs for slow neutrons ($E_n = 2 \text{ meV}$) if they would have been converted only in the last layer. Considering the conversion probability in each layer, it can be shown that the average contribution to the uncertainty of the TOF is about 6.5 μs .

The count rate detector stability during a long period of measurements has been estimated taking into account a run series performed during 8 h. Each run has been normalised for the run time (about 70 s); then, the total counts of all runs have been normalised for a reference run Fig. 9 and reported in the histogram in Fig. 10. Fitting such a histogram with a simple Gaussian distribution, the FWHM is 1% which means that the detector is stable at 99% during a long period of measurements. The main parameter that affects the measurements is the current instability of the proton beam of ISIS; in fact, all measurements have been normalised to this parameter. To estimate how the I-MS-BGEM detector is sensitive with respect to the ISIS beam current fluctuations, the proton beam current values (provided by the diagnostics of the ISIS accelerator¹¹ have been histogrammed and then reported in Fig. 11. The obtained parameters from the Gaussian fit of the plot in Fig. 11 highlight that the FWHM (1.12 μA) normalised for the centroid is 1%. In conclusion, the measurements provided by the I-MS-BGEM detector are stable and the instability of 1% is mostly due to the instability of the beam current (Fig. 11).

A comparison of the detectors features (of the ³He, ⁶Li based scintillator and I-MS-BGEM) are reported inside the Table 1.

As mentioned in the introduction, the ³He is limited on the counting rate capability; although it is very efficient to perform spectroscopy or diffraction experiments, if it would be installed directly into the neutron beam a detector saturation will occur. The ⁶Li-glass scintillator is designed to be capable to sustain high neutron fluxes and to have a stable counting rate during long measurement time, but it is sensitive to photons²¹. With the I-MS-BGEM detector, the detection efficiency reaches a value of 16% at thermal neutrons sustaining a counting rate capability in the order of MHz; moreover, it is stable (99%, for 8 h measurement, see Fig. 9) with a good capability to discriminate the events due to the neutron interaction from gamma background (see Fig. 8).

Conclusions

The work presented in this paper shows the performances of the I-MS-BGEM detector. The device has been tested at the VESUVIO beamline with thermal/epithermal neutrons at the ISIS Pulsed Neutron and Muon Source.

The performed measurements have highlighted the good capability to discriminate gamma rays from neutrons with a value of $(1.07 \pm 0.05) \times 10^{-5} \frac{\text{c}}{\text{n}}$. The detection efficiency increases with the wavelength, as expected in the ideal case in which the efficiency is dominated by the neutron conversion probability in boron, without sign of losses of signal. The measured efficiency resulted to be 16% at 1.8 \AA up to 50% at 6 \AA for a 6 BGEMs stack, a significant improvement with respect to the previous GEM-based VESUVIO detector²². The detector count rate resulted to be in the order of 99%, and the 1% instability is due to the ISIS proton beam current fluctuations.

During the measurements, the I-MS-BGEM sustained the full VESUVIO neutron flux (reaching an average counting rate of 1.5 MHz) without sign of event losses.

The capability to sustain a high neutron flux and to discriminate the neutrons from gamma rays combined with the good detection efficiency (even increasable with the addition of further BGEM foils), and the good time resolution, make the I-MS-BGEM detector a unique device for the neutron techniques requiring such features. In particular, its use can easily be envisaged in techniques involving transmission neutron measurements, that are characterised by high fluxes impinging on the detectors and a high background, with the added bonus of a 2D-resolved capability due to the padded anode.

Data availability

The dataset generated and/or analysed during the current study are available from the corresponding author on reasonable request.

Received: 16 May 2024; Accepted: 30 September 2024

Published online: 14 October 2024

References

1. Knoll, G. *Radiation Detection and Measurement* (John Wiley, 2010).
2. Shea, D. & Morgan, D. *The Helium-3 Shortage: Supply, Demand, and Option for Congress* (Congressional Research Service, 2010).

3. Falahat, S. *et al.* A ^3He neutron detector for the measurement of (α , n) reactions. *Nucl. Inst. Methods Phys. Res. A* **700**, 53–58. <https://doi.org/10.1016/j.nima.2012.10.036> (2013).
4. Sauli, F. The gas electron multiplier (GEM): Operating principles and applications. *Nucl. Inst. Methods Phys. Res. A* **805**, 2–24. <https://doi.org/10.1016/j.nima.2015.07.060> (2016).
5. Croci, G. *et al.* GEM-based thermal neutron beam monitors for spallation sources. *Nucl. Inst. Methods Phys. Res. A* **732**, 217–220. <https://doi.org/10.1016/j.nima.2013.05.111> (2013).
6. Klein, M. & Schmidt, C. J. CASCADE, neutron detectors for highest count rates in combination with ASIC/FPGA based readout electronics. *Nucl. Inst. Methods Phys. Res. A* **628**(1), 9–18. <https://doi.org/10.1016/j.nima.2010.06.278> (2011).
7. Kohli, M. *et al.* CASCADE-a multi-layer Boron-10 neutron detection system. *J. Phys. Conf. Ser.* <https://doi.org/10.1088/1742-6596/746/1/012003> (2016).
8. Höglund, C. *et al.* B4C thin films for neutron detection. *J. Appl. Phys.* <https://doi.org/10.1063/1.4718573> (2012).
9. Muraro, A. *et al.* MBGEM: A stack of borated GEM detector for high efficiency thermal neutron detection. *Eur. Phys. J. Plus* <https://doi.org/10.1140/epjp/s13360-021-01707-2> (2021).
10. Patra, R. N. *et al.* Measurement of basic characteristics and gain uniformity of a triple GEM detector. *Nucl. Inst. Methods Phys. Res. A* **862**, 25–30. <https://doi.org/10.1016/j.nima.2017.05.011> (2017).
11. <http://www.isis.rl.ac.uk/>.
12. Romanelli, G. *et al.* Characterisation of the incident beam and current diffraction capabilities on the VESUVIO spectrometer. *Meas. Sci. Technol.* <https://doi.org/10.1088/1361-6501/aa7c2a> (2017).
13. Robledo, J. I. *et al.* Measurement of neutron total cross sections at the VESUVIO spectrometer. *Nucl. Inst. Methods Phys. Res. A* **971**, 164096. <https://doi.org/10.1016/j.nima.2020.164096> (2020).
14. <https://home.cern/>.
15. <https://europeanspallationsource.se/>.
16. Pezzotta, A. *et al.* GEMMA and GEMINI, two dedicated mixed-signal ASICs for Triple-GEM detectors readout. *J. Instrum.* **11**(03), C03058–C03058. <https://doi.org/10.1088/1748-0221/11/03/C03058> (2016).
17. Cancelli, S. *et al.* Electronic readout characterisation of a new soft X-ray diagnostic for burning plasma. *J. Instrum.* **17**(08), C08028. <https://doi.org/10.1088/1748-0221/17/08/C08028> (2022).
18. Wilson, C. C. ISIS, the UK spallation neutron source - a guided tour. *Neutron News* **1**(1), 14–19. <https://doi.org/10.1080/10448639008210192> (1990).
19. Senesi, R. *et al.* VESUVIO: A novel instrument for performing spectroscopic studies in condensed matter with eV neutrons at the ISIS facility. *Phys. B Phys. Condens. Matter* **276**, 200–201. [https://doi.org/10.1016/S0921-4526\(99\)01246-6](https://doi.org/10.1016/S0921-4526(99)01246-6) (2000).
20. <https://www.nds.iaea.org/>.
21. <https://scintacor.com/technologies/neutrons/>.
22. Cancelli, S. *et al.* Development of a ceramic double thick GEM detector for transmission measurements at the VESUVIO instrument at ISIS. *J. Instrum.* <https://doi.org/10.1088/1748-0221/16/06/P06003> (2021).
23. Romanelli, G. *et al.* Thermal neutron cross sections of amino acids from average contributions of functional groups. *J. Phys. Condens. Matter* <https://doi.org/10.1088/1361-648X/abfc13> (2021).
24. Leinweber, G. *et al.* Cadmium resonance parameters from neutron capture and transmission measurements at the RPI LINAC. <https://doi.org/10.48550/arXiv.1801.03424> (2018).

Acknowledgements

In memory of Dr. Fabrizio Murtas, who passed away in 2022. He was the first proposer of this project.

Author contributions

G.C. and A.M. conceptualized the study. S.C., O.P., A.C. and F.C. developed the experimental setup. S.C., E.P.C., O.P., G.R. and M.K. performed the experiments. S.C. and F.C. performed the data analysis. S.C. drafted the manuscript. G.C., E.P.C., M.T., S.R.P. and G.G. revised the manuscript. All authors have read and approved the final version of the manuscript for publication and agreed to be accountable for their contributions.

Declarations

Competing interests

The authors declare no competing interest.

Additional information

Correspondence and requests for materials should be addressed to S.C.

Reprints and permissions information is available at www.nature.com/reprints.

Publisher's note Springer Nature remains neutral with regard to jurisdictional claims in published maps and institutional affiliations.

Open Access This article is licensed under a Creative Commons Attribution-NonCommercial-NoDerivatives 4.0 International License, which permits any non-commercial use, sharing, distribution and reproduction in any medium or format, as long as you give appropriate credit to the original author(s) and the source, provide a link to the Creative Commons licence, and indicate if you modified the licensed material. You do not have permission under this licence to share adapted material derived from this article or parts of it. The images or other third party material in this article are included in the article's Creative Commons licence, unless indicated otherwise in a credit line to the material. If material is not included in the article's Creative Commons licence and your intended use is not permitted by statutory regulation or exceeds the permitted use, you will need to obtain permission directly from the copyright holder. To view a copy of this licence, visit <http://creativecommons.org/licenses/by-nc-nd/4.0/>.

© The Author(s) 2024